Simulating Atmosphere-Fire Interactions using a Coupled Weather – Wildland Fire Model

Kartsios S.[1*], Karacostas Th.[1], Pytharoulis I.[1], Dimitrakopoulos A.P.[2]

[1] *Department of Meteorology and Climatology, School of Geology, Faculty of Sciences, Aristotle University of Thessaloniki, Thessaloniki, Greece.*
[2] *Department of Forestry and Natural Environment, Aristotle University of Thessaloniki, Thessaloniki, Greece.*
[*]*corresponding author e-mail: kartsios@geo.auth.gr*

Abstract Atmosphere – fire interactions play a significant role in fire behavior since, during a wildland fire, physical processes concurrently occur in different scales. In this study, the Coupled Weather – Wildland Fire Model, WRF-SFIRE, was used in order to simulate a wildland fire. The input data consisted of theoretical vertical profiles of potential temperature and water vapor mixing ratio up to 2 km height, a uniform westerly wind field, surface pressure and custom fuel values (representative of the Greek natural environment and based on actual field measurements) in a flat and uniform terrain. The atmospheric model, configured in turbulence-resolving large-eddy-simulation (LES) mode, produced ideal simulations at a horizontal resolution of 50 m and 5 m for the WRF and the SFIRE models, respectively. Simulations were carried out within a forecast horizon of 2.5 hours. Point ignition was chosen and the fire was allowed to spread freely due to fire-atmosphere feedbacks. Results showed that the simulated fire burned in a narrow ellipse shape, generating a well-defined pyro-convective plume, due to sensible and latent heat fluxes that were produced from the fire. Due to intense heating, the maximum instantaneous total released sensible heat fluxes were 41 GW while vertical velocities reached up to 35 ms^{-1}. Fire-induced surface flow led to maximum horizontal winds of 29 ms^{-1} (10 m above the ground), ahead of the fire-front. Atmosphere – fire dynamics seem to be adequately simulated by the model, as evidenced by a convergence region, observed in front of the fire-line and associated with a pair of strong positive and negative vertical vorticity with maxima of ~0.1 s^{-1}. However, this dynamic characteristic was transient due to the highly disturbed background flow. Conclusively, the WRF-SFIRE model seem to have the potential for realistic simulation of the atmosphere – fire interactions and ultimately, it can be a useful tool with the proper adjustments for fire behavior monitoring and fire suppression planning.

Keywords
Weather, wildland fires, forest fuels, WRF-SFIRE, Evergreen-sclerophyllous shrublands, Mediterranean vegetation types.

Introduction

Weather is the most variable and less predictable factor in the vicinity of the fire, while it may affect the fuel properties and general fire behavior (Whiteman, 2000; Potter, 2012a,b). Along with meteorological conditions, topography and fuel properties are also the key factors during a wildland fire, since a change in any one of these elements will cause a change in the behavior of the fire.

Wildland fire modeling ranges from numerical fire prediction systems based on equations that describe the physical and chemical processes in atmosphere-fire interactions, to either empirical algorithms, which are based on phenomenological or statistical description of fire behavior (Kochanski et al., 2013). WRF-SFIRE (Mandel et al. 2011) can be categorized as "quasi" coupled atmosphere-fire model, where the physics of coupled atmosphere-fire are included but heat and moisture release rates, fuel consumption and fire spread rate are obtained from prescribed formulae or semi-empirical relations.

Fuel models are used as inputs in fire behavior prediction systems, as they simulate fuel elements with average fuel properties values representative of the typical fuel conditions of a certain vegetation type (Burgan and Rothermel, 1984; Dimitrakopoulos, 2002). As an example, in USA, thirteen (13) fuel categories are used in BEHAVE fire behavior prediction system (Andrews, 1986). Dimitrakopoulos et al. (2001) and Dimitrakopoulos (2002) introduced seven (7) fuel models that were developed from the

Mediterranean vegetation types of Greece and estimated their potential fire behavior according to BEHAVE simulations.
In this study, the Evergreen-sclerophyllous shrublands (maquis) (1.5 up to 3.0 m) fuel model (Dimitrakopoulos, 2002), representative of the Greek natural environment is used for the first time as input to WRF-SFIRE, in order to represent a highly idealized wildland fire and evaluate the ability of the model to simulate adequately the atmosphere-fire interactions, using a custom fuel model beyond default fuel configuration.

Methodology

For the purposes of this study, the non-hydrostatic Weather Research and Forecasting model with the Advanced Research dynamic solver (WRF-ARW Version 3.4) was initialized in the ideal simulation (Wang et al., 2012) and configured in turbulence-resolving large-eddy-simulation (LES) mode. At the surface, each atmospheric grid cell is divided into two-dimensional fuel cells, where rate of spread (ROS) and post-frontal sensible and latent heat fluxes are calculated from the fire (SFIRE) model. The heat fluxes from the fire are inserted into the atmospheric model as forcing terms in the differential equations of the atmospheric model into a layer above the surface, with assumed exponential decay with altitude (Mandel et al. 2011). The WRF-SFIRE's source code was obtained from the Open Wildland Fire Modeling E community (openWFM.org), which is frequently updated by the developers. A restricted version is available in WRF releases, referred as WRF-Fire.
The single model domain configuration follows Kartsios et al. (2014), with a west-east and south-north extent of 7.5 km and a uniform and flat terrain. Model top was placed at 2 km as in Jenkins et al. (2011), Coen et al. (2013) and Kochanski et al. (2013). The horizontal grid spacing in x-y dimensions was 50 m. A hyperbolically-stretched vertical grid was used (40 levels, with the first 30 levels under 1 km), defining a computational domain of 150 x 150 x 40 (x,y,z) grid points. Using this hyperbolically-stretched vertical grid, the first model level was set approximately at 3.5 m and the second at 11 m, as the fire model uses the wind speed interpolated to 6.1m above the ground. The model time step was 0.2 s, for preventing unstable numerical solutions, while open boundary conditions were applied on the lateral boundaries. Atmosphere to fire refinement ratio was 10, which implies a grid spacing of 5 m for the SFIRE model. This fine horizontal discretization for the fire grid is necessary for proper feedback of the wind on the fire line (Mandel et al., 2011). Only the MM5 surface layer scheme, based on Monin–Obukhov similarity and the 5-layer surface model (SLAB 5-layer MM5 model, Skamarock et al. 2008), were activated, while the rest of physics schemes, such as microphysics, longwave and shortwave radiation, planetary boundary layer and cumulus parameterization were disabled.
The ideal atmosphere in which the fire ignites was constructed according to theoretical vertical profiles of potential temperature (θ) and water vapor mixing ratio (r) up to 2 km height (Fig. 1a,b), as in Kartsios et al. (2014). At surface (at first model time step), the pressure was 1015 hPa, temperature was set to 303 K and water vapor mixing ratio was 12 gkg^{-1}. A uniform westerly wind field of 4 ms^{-1} was set at the western lateral boundary. The full surface initialization option was enabled and the skin surface temperature was set to 307 K while the mean soil temperature to 302.7 K. The latter values were obtained from observation data of the 8th August of 2012 at the conventional meteorological station of Aristotle University of Thessaloniki and adapted to the ideal atmosphere just to represent actual soil temperature measurements.

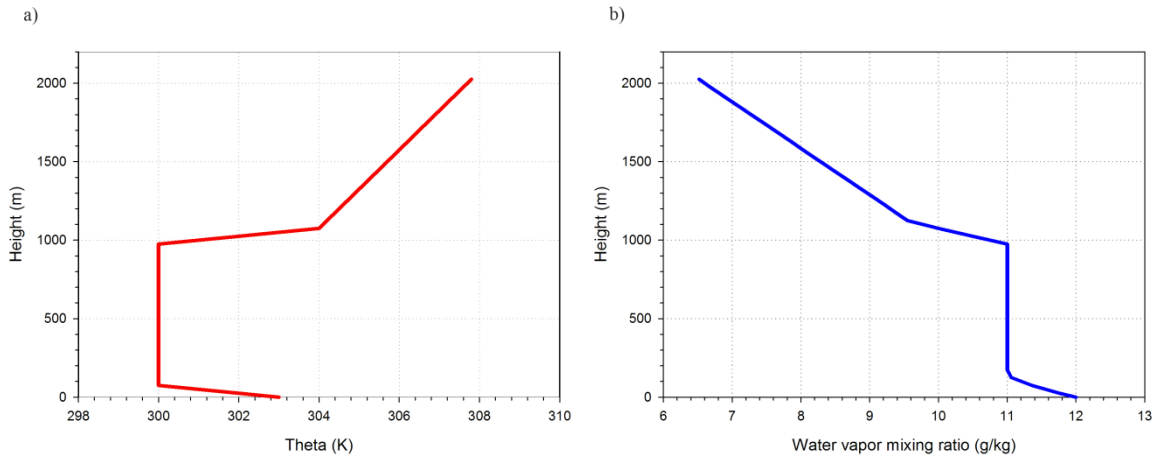

Figure 1. Vertical distributions or potential temperature (a) and water vapor mixing ratio (b) as input data during WRF's initialization.

For the initialization of SFIRE model, fuel properties must be provided, in order to be interpolated into the fire grid. Anderson's thirteen (13) fuel categories (Anderson, 1982) are considered as the default configuration. However, in this study, custom fuel values, based on actual field measurements from Greece, were assigned across the entire model domain (Tab. 1). These values represent a Mediterranean shrubland (maquis) fuel model, named Evergreen-sclerophyllous shrublands (1.5 up to 3.0 m), which was resulted from the cluster analysis that represents all the major Mediterranean vegetation types of Greece (Dimitrakopoulos et al., 2002). The methodology for the development of the particular fuel model can be found in Dimitrakopoulos et al. (2002). The fire ignition took place 1830 s (30.5 min) after the start of the simulation, with the first 30 min accounted as spin up period. Point ignition, at point A(1850m, 3750m) from the domain's lowest left corner, was chosen as ignition mechanism and the fire spread freely for the remaining 2 hours, due to the two-way coupling between the atmospheric and fire model. Simulation results were stored in 10 min intervals.

Table 1. Fuel properties of Dimitrakopoulos' et al. (2002) fuel model, Evergreen-sclerophyllous shrublands (1.5 up to 3.0 m). The identifiers are as used in SFIRE (Mandel et al., 2011).

Symbol	*Description*	*Identifier*	*Value*
α	Wind adjustment factor	windrf	0.78
z_f	Fuel wind height (m)	fwh	3.0
z_0	Fuel roughness height (m)	fz0	0.2834
w	Fuel weight (s)	weight	3.4
w_l	Total fuel load (kgm^{-2})	fgi	4,908
δ_m	Fuel depth (m)	fueldepthm	2.18
σ	Fuel particle surface-area-to-volume ratio (m^{-1})	savr	1600
M_x	Moisture content of extinction (%)	fuelmce	0.35
ρ_P	Ovendry fuel particle density (kgm^{-3})	fueldens	32
S_T	Fuel particle total mineral content	st	0.0555
S_E	Fuel particle effective mineral content	se	0.010
h	Fuel heat contents of dry fuel (Jkg^{-1})	cmbcnst	17433000
M_f	Fuel particle moisture content	fuelmc_g	0.016

Results and Discussion

Evergreen-sclerophyllous shrublands (1.5 up to 3.0 m) fuel model is characterized by maximum values of fire-line intensity and rate of spread. Dimitrakopoulos et al. (2002) carried out fire simulations with BEHAVE model (Andrews, 1986) and found that the shrubland fuel models have the most severe fire potential due to heavier fuel loads (their Tab. 2). During the entire simulation the maximum rate of spread in the normal direction to the fire-line was 4.8 ms^{-1} while the maximum fire-line intensity was 319.1 MWm^{-1}. The aforementioned values were recorded at the same time interval, 40 min after the ignition.

In figure 2, the instantaneous total released sensible heat fluxes (MW) for the entire domain are presented with maximum at 41 GW, 40 min after the ignition. Two major outbreaks can be shown, the first one starting approximately one hour after the onset of the simulation and the second one appearing at the end. The total burned area was 1.03 km^2, as it is shown in figure 2. Clearly, there is a connection between the first outbreak of total released sensible heat fluxes and the rate of burned area's growth. This change of fire's growth is attributed to higher surface winds generated from high temperature gradients between the fire-line and the unburned area. The maximum wind speed at 10m was 29 ms^{-1} and it was located in front of the fire-line.

Figure 3 shows maximum sensible heat fluxes from ground fire (kWm^{-2}) (red solid line) and maximum values of vertical w-wind component (ms^{-1}) (blue dashed line) for the entire simulation. Due to intense heating during these aforementioned outbreaks, maximum vertical velocities reached 34.9 ms^{-1} and 27.7ms^{-1}, respectively (Fig. 3), enhancing further the already existed pyro-convection, while the total maximum sensible heat fluxes produced by the fire were 1450 kWm^{-2}. Generally, strong updrafts appeared during the entire simulation, at middle and higher levels, indicating a very strong pyro-convective plume, and as a result a plume-driven fire.

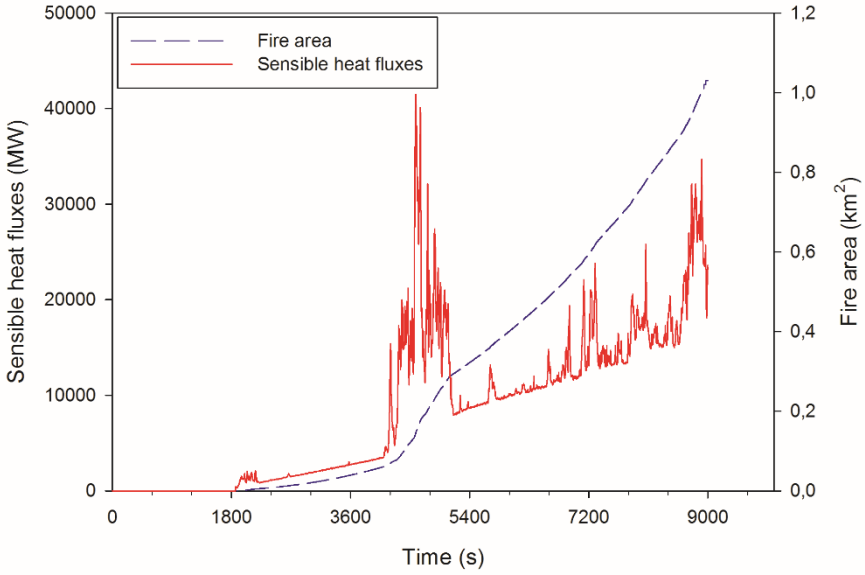

Figure 2. Accumulated released sensible heat fluxes (MW) for the entire domain in each time step (red solid line) and burned area (km^2) (blue dashed line), for the entire simulation.

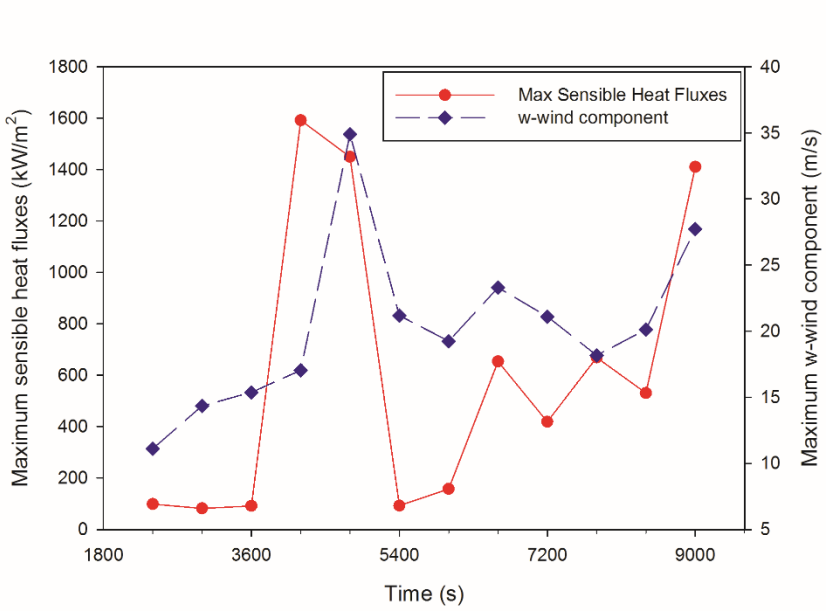

Figure 3. Maximum sensible heat fluxes from ground fire (kWm^{-2}) (red solid line) and maximum values of w wind component (ms^{-1}) (blue dashed line).

The pyro-convective plume was well defined (Fig. 4a,b) and was limited by the model's top. A vertical circulation was shown up at higher model levels and it was generated because of the limitations in domain's vertical extent. The limited vertical extension of the domain suppressed the potential development of the pyro-convective plume, which affected at some point, the thermodynamic processes. Work on progress is trying to estimate the sensitivity of this vertical circulation with the model top. Moreover, the uniform westerly flow was unable to tilt the vertical axis of the pyro-convective column at that moment, while the entrainment of colder ambient air into the plume should be emphasized.

The intense burning increased the air temperature inside the fire plume. In figure 4b, the isotherm of 24 ^{o}C can be shown, where in areas with no fire burning below, it is located ~400 m above ground level (e.g. at 1 km in west-east direction), while in areas with intense heating it appears at ~1200m a.g.l. This temperature increase results in decreased relative humidity inside the pyro-convective plume (Fig. 4b), until middle levels. As the warm air ascended and reached at higher levels, it was adiabatically cooled and the relative humidity increased above 90%.

Kochanski et al. (2013) used WRF-SFIRE in order to validate model's ability in simulating, among others, the temporal change in air temperature before and after the passage of the fire-front. They showed overall, good agreement between observed and simulation data. In lack of observation data, we are unable to perform such analysis but to demonstrate how the model simulated the front passage. Figure 5 depicts time series of air temperature at location B(2025m, 3775m) from domain's bottom left corner, at 15 m (dots), 40 m (open circles) and 80 m (triangles) a.g.l. As it is shown in figure 5, the model simulated the fire-front passage at location B, where air temperature began to rise above ambient temperature values and fell as the fire-front passed. The increase in temperature occurred first at higher levels, indicating a tilted plume structure (Fig. 4), as was observed in Clements (2010). Note the small decrease in temperature values at 15 m (dots), as the fire-front approached. This cooling may be attributed to one extent to the entrainment of colder ambient air due to the convergence zone at surface, in front of the fire-front (Clark et al., 1996a). Similar behavior was observed during Fireflux (Clements et al., 2007, their fig. 6). In addition, as air rises, the rapid change in pressure activates the dry adiabatic cooling mechanism, which is described by the equation,

$$\frac{dT}{T} = \frac{Rd}{Cp} \cdot \frac{dP}{P} \quad , (1)$$

where T is the temperature, P is the pressure, Rd is the specific gas constant of dry air and Cp is the specific heat at constant pressure.

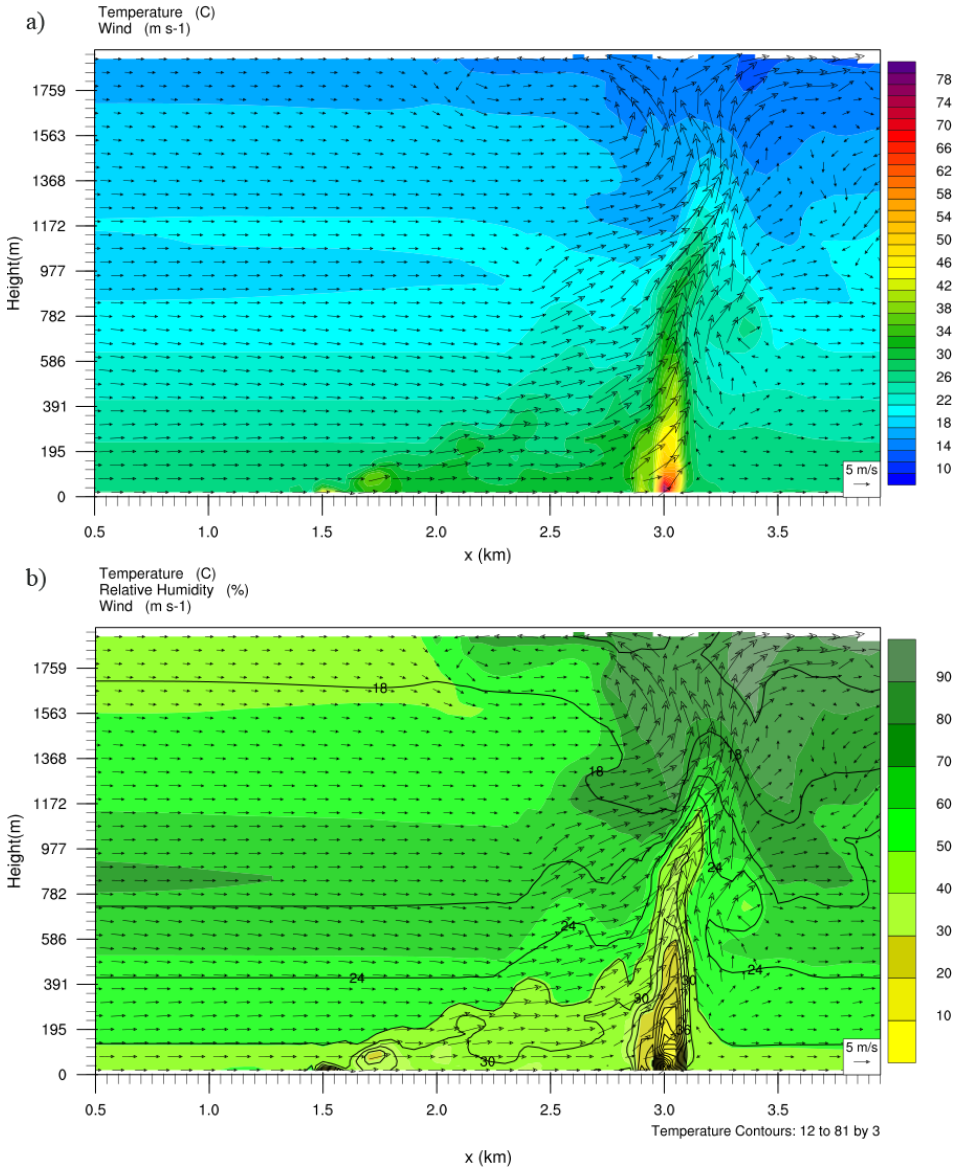

Figure 4. Vertical distributions of temperature (^{o}C; shading) and wind (ms^{-1}; vectors) in (a), temperature (^{o}C; contours), relative humidity (%; shading) and wind (ms^{-1}; vectors) in (b), 2.5 h since the onset of the simulation. Wind distribution was determined using u and w wind components. The vertical cross-section was considered through the middle of y axis.

It must be mentioned that the level of 15 m a.g.l. was considered as the heat extinction depth equal to flame heights, which is the top height in which the transport of sensible, latent and radiant heat from the fire's combustion into the lowest levels of WRF model occurs. It seems that this heat extinction depth variable is connected with temperature behavior at lowest model levels, where during sensitivity runs, greater values produced smaller heating at the surface, while small values resulted in greater temperature values but also in strong cooling, which was unexpected. After the front passage air temperature was slightly higher than the pre-fire values, indicating that the remaining fuel was still on fire.

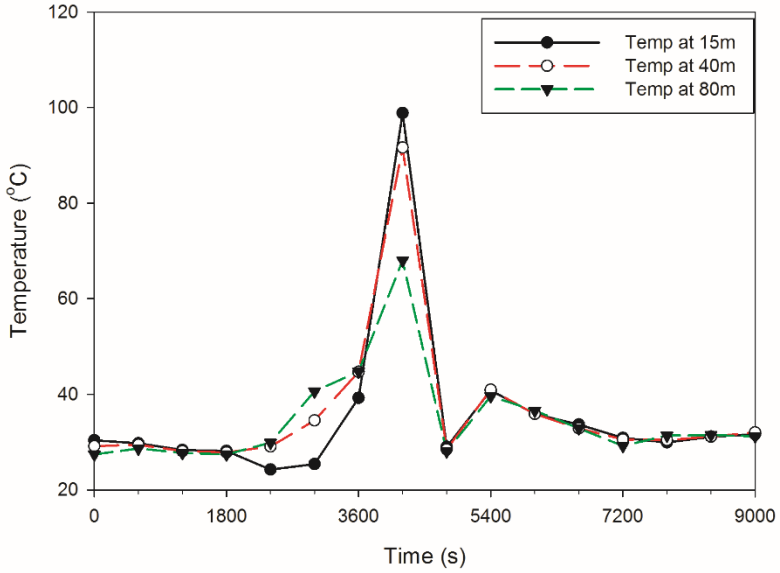

Figure 5. Temporal change of air temperatures at point location B(2025m,3775m) from domain's bottom left corner, at 15 m (dots), 40 m (open circles) and 80 m (triangles) a.g.l. (above ground level).

WRF-SFIRE model was able to capture and analyze atmosphere-fire dynamics, as well. In figure 6, the vertical component of relative vorticity in x-y plane is presented, 1 h and 50 min after the ignition at 10 m (a), 50 m (b), 100 m (c), 200 m (d), 500 m (e) and 1000 m (f) above surface. A strong anticyclonic vortex of negative vertical vorticity (~0.14 s^{-1}) accompanied by a smaller in magnitude cyclonic vortex of positive vertical vorticity is evident in fire-front (arrows in Fig. 6a). Couplets of cyclonic and anticyclonic vortices, located in fire-front, are described also by Clark et al. (1996a,b) and Jenkins et al. (2011).

The above-mentioned couplet is vertically extended and amplified in magnitude as the height increases (Fig. 6b,c). In particular, the cyclonic vortex of positive vertical vorticity, which was not so distinct near surface, is well organized at these levels (50-100 m a.g.l.). Note that the vertical axis of the vortices is tilted eastwards with height, due to westerly background flow. Pairs of clockwise and counter-clockwise vortices are present at 200 m and 500 m (Fig. 6d,e), some of which are the vertical extension of the aforementioned vortices, while at 1000 m a.g.l (Fig. 6f), new vortices are appearing, with maxima of negative vorticity nearly at 0.15 s^{-1}. Above that level, the strength and the magnitude of the vortices are decreasing as the height increases.

Although a convergence region ahead of the fire-line appeared during the simulation as in Kartsios et al. (2014), it was not so distinct due to highly perturbed background flow (not shown). This near surface convergence pattern at the vicinity of fire acts as propagation mechanism according to Clark et al. (1996a). Strong convergence in surface flow was presented also at the flanks of the fire area and at the tip and ahead of the burning fire-front.

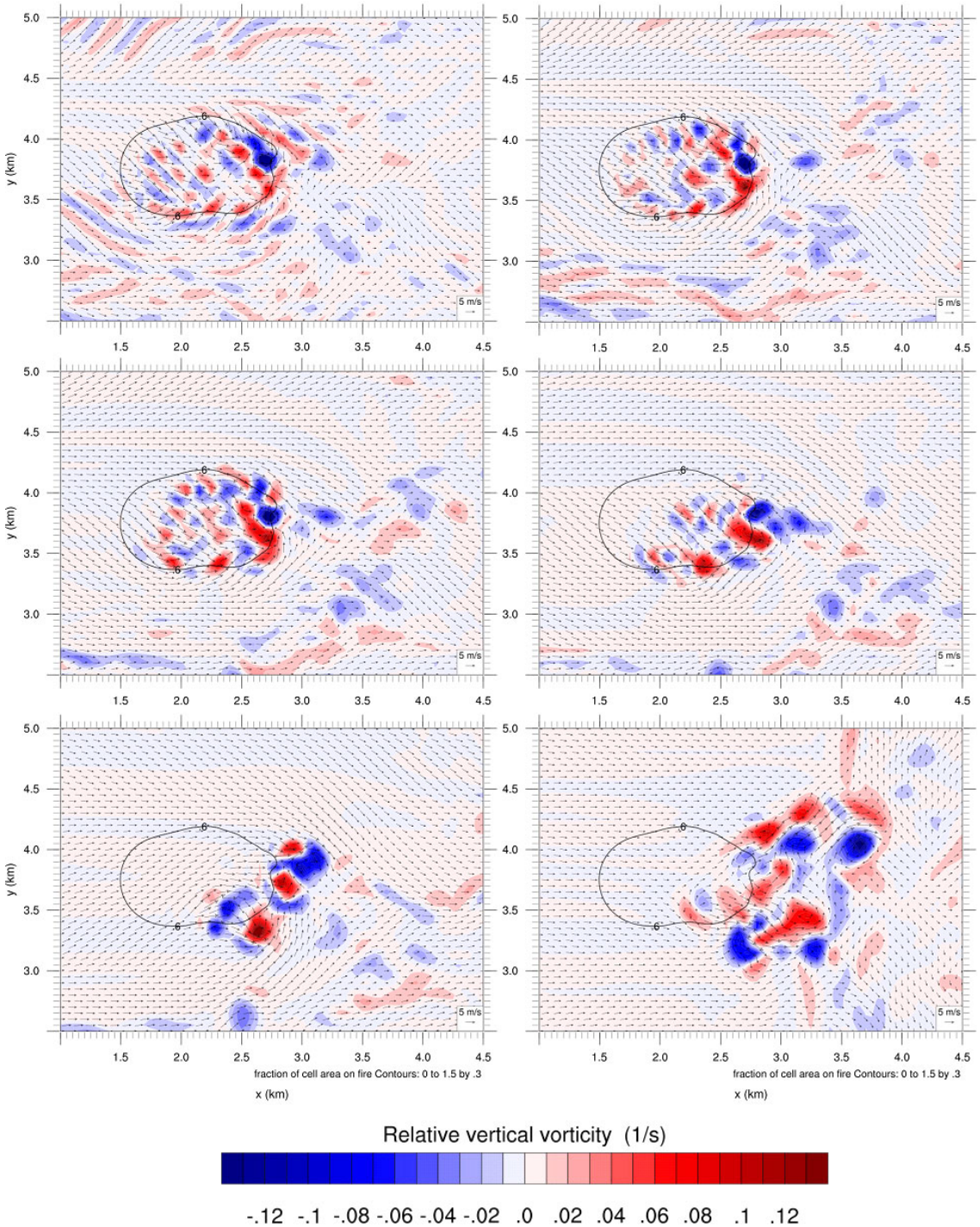

Figure 6. Vertical component of relative vorticity,1 h and 50 min after the ignition at 10 m (a), 50 m (b), 100 m (c), 200 m (d), 500 m (e) and 1000 m (f) above surface (contours). Wind vectors are calculated at the aforementioned heights. Solid line represents fire area at surface. The depicted domain is zoomed from the original for better representation.

Conclusions

In this study, custom fuel properties, representative of the Greek natural environment and based on actual field measurements were imported for the first time into WRF-SFIRE modeling system, in order to

represent a wildland fire. Through idealized atmospheric forcing, a description of atmosphere-fire interactions was attempted by examining certain atmospheric and fire variables. The fuel model produced both great values of rate of spread and fire-line intensity, confirming previous studies about the potential fire behavior of this fuel type. Rate of fire area's growth was connected with the release of heat fluxes from the burning fuels, which in turn affected the magnitude of the vertical velocities due to intense heating. A well-defined pyro-convective plume appeared, while the thermal plume structure was simulated by the model. Although the model represented adequately the fire-front passage, the effect of heat extinction depth variable (the transport of sensible, latent and radiant heat from the fire's combustion into the lowest levels of WRF) on near surface temperatures must be mentioned. Flow dynamics were captured and analyzed with couplets of cyclonic and anticyclonic vortices located in fire-front and ahead, with -tornado strength- nearly equal maxima of positive and negative vertical vorticity. Conclusively, the WRF-SFIRE modeling system seems to have the potential for realistic simulation of the atmosphere – fire interactions establishing it as a useful tool in fire behavior monitoring and fire suppression planning.

Acknowledgments
The authors would like to thank the National Center for Atmospheric Research (NCAR) for providing WRF-ARW model and also the Open Wildland Fire Modeling E community for their support and guidance in WRF-SFIRE modelling system.

References

Anderson H.E., 1982. Aids to determining fuel models for estimating fire behavior. USDA Forest Service, Intermountain Forest and Range Experiment Station, General Technical Report INT-122. 22 p., available at: http://www.fs.fed.us/rm/pubs_int/int_gtr122.html.

Andrews P.L., 1986. BEHAVE: fire behavior prediction and fuel modeling system – BURN subsystem, Part 1. USDA Forest Service, Intermountain Research Station General Tenchical Report INT-194. Ogden, UT. 130pp.

Burgan R.E. and Rothermel R.C., 1984. BEHAVE: fire behavior prediction and fuel modeling system – Fuel subsystem. USDA Forest Service, Intermountain Research Station General Tenchical Report INT-167. Ogden, UT. 126pp.

Clark T.L., Jenkins M.A., Coen J. and Packham D., 1996a. A coupled atmosphere-fire model: Convective feedback on fire–line dynamics. *J Appl Meteor.*, 35:875–901.

Clark T.L., Jenkins M.A., Coen J. and Packham D., 1996b. A coupled atmosphere-fire model: Role of the convective froude number and dynamic fingering at the fireline. *Int. J. Wildland Fire*, 6, 177–190.

Clements C. B., Zhong S., Goodrick S., Li J., Potter B. E., Bian X. and Heilman W. E., 2007. Observing the dynamics of wildland grass fires: FireFlux - A field validation experiment. *Bull. Amer. Meteor. Soc.*, 88 (9), 1369-1382. doi: 10.1175/BAMS-88-9-1369.

Coen J., Cameron M., Michalakes J., Patton E., Riggan P. and Yedinak K., 2013. WRF-SFIRE: Coupled Weather-Wildland Fire Modeling with the Weather Research and Forecasting Model. *J Appl Meteor Climatol.*, 52:16-38. doi:10.1175/JAMC-D-12-023.1.

Dimitrakopoulos A.P., Mateeva V. and Xanthopoulos G. 2001. Fuel models of Mediterranean vegetation types in Greece. *Geotechnical Scientific Issues*, Issue VI, 12 (3), 192-206 (In Greek).

Dimitrakopoulos A.P., 2002. Mediterranean fuel models and potential fire behavior in Greece. *Int. J. Wildland Fire*, 11, 127-130.

Jenkins M.A., Kochanski A.K. and Krueger S.K., 2011. The fluid dynamics of steady-state fireline propagation. *Ninth Symposium on Fire and Forest Meteorology*, Palm Springs, CA, October 18-20.

Kartsios S., Karacostas Th., Pytharoulis I., and Dimitrakopoulos A.P., 2014. Coupled Weather – Wildland Fire Model for fire behavior interpretation. *Proceedings of the 12th on Meteorology, Climatology and Atmospheric Physics*, 28-31 May, Heraklion, Greece, 478-482.

Kochanski A.K., Jenkins M.A., Mandel J., Beezley J.D., Clements C.B. and Krueger S., 2013. Evaluation of WRF-SFIRE performance with field observations from FireFlux experiment. *Geosci Model Dev*, 6:1109–1126. doi: 10.5194/gmd-6-1109-2013.

Mandel J., Beezley J.D. and Kochanski A.K., 2011. Coupled atmosphere-wildland fire modeling with WRF 3.3 and SFIRE 2011. *Geosci Model Dev*, 4:591–610. doi:10.5194/gmd-4-591-2011.

Potter B.E., 2012a. Atmospheric interactions with wildland fire behavior - I. Basic surface interactions, vertical profiles and synoptic structures. *Int. J. Wildland Fire*, 21, 779-801.

Potter B.E., 2012b, Atmospheric interactions with wildland fire behavior – II. Plume and vortex dynamics. *Int. J. Wildland Fire*, 21, 802-817.

Skamarock W.C., Klemp J.B, Dudhia J., Gill D.O., Barker D.M., Duda M.G., Huang X.-Y., Wang W. and Powers J.G., 2008. A Description of the Advanced Research WRF Version 3, NCAR Technical Note 475, available at: http://www.mmm.ucar.edu/wrf/users/docs/arw v3.pdf.

Wang W., Bruyère C., Duda M., Dudhia J., Gill D., Lin H.C., Michalakes J., Rizvi S., Zhang X., Beezley J.D., Coen J.L., Mandel J., Chuang H.-Y., Mckee N., Slovacek T. and Wolff J., 2012. ARW Version 3 Modeling System User's Guide, Mesoscale & Miscroscale Meteorology Division, National Center for Atmospheric Research, 384pp.

Whiteman C.D., 2000. *Mountain meteorology: Fundamentals and Applications*. Oxford University Press, New York, 355pp.